POLITECNICO
MILANO 1863

PEEC Method Applied to Rectangular Conductors

Computational Electromagnetics

Filippo Rigoni

March 14, 2025

PEEC Method Applied to a Rectangular Conductor

Consider a non-magnetic straight rectangular conductor $\Gamma(l, w, t)$ with length l, width w and thickness t.
$\Gamma(l, w, t)$ is located in free space with permeability μ_0 and carries a time-harmonic current $i(t) = \mathcal{R}(\underline{\mathbf{I}} \cdot e^{j\omega t})$ parallel to its axis.
The current amplitude $|\underline{\mathbf{I}}|$ and angular frequency $\omega > 0$ are given.

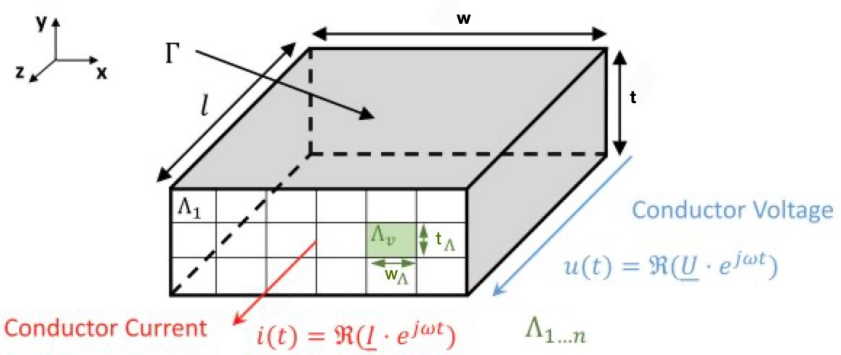

Figure 1: Rectangular conductor Γ subdivided into n current filaments Λ.

A Cartesian coordinate system (x, y, z) is introduced where the z-axis is parallel to the current flow direction.
κ_Γ is the conductivity of the conductor and outside Γ is zero.

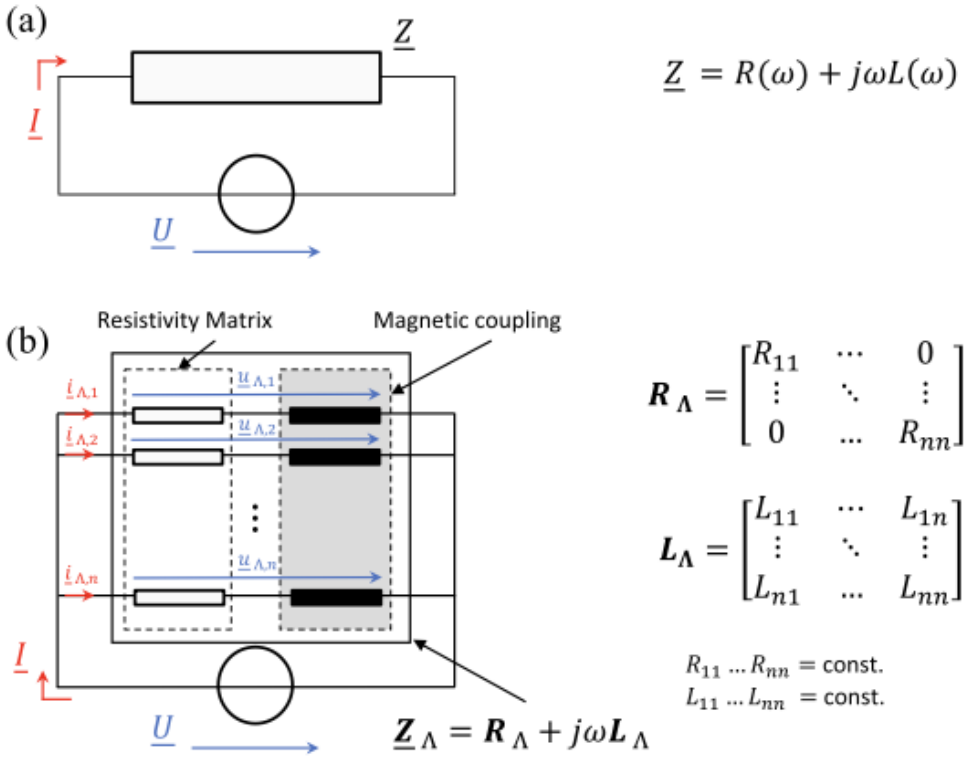

Figure 2: Equivalent electrical circuit of (a) conductor as a single element and (b) conductor subdivided into parallel filaments.

Fig. 2 shows how the **terminal quantities**, voltage and current, of the conductor can be described by a complex impedance $\underline{\mathbf{Z}}$, that will be frequency-dependent:

$$\underline{\mathbf{Z}} = R + j\omega L \tag{1}$$

To calculate $\underline{\mathbf{Z}}$, the conductor is subdivided into n **uniform** smaller filaments, $\Gamma_1, \ldots, \Gamma_n$.
The extensions t_Λ and w_Λ of these filaments perpendicular to the z-axis are chosen such that $t_\Lambda, w_\Lambda \ll \delta$ holds, so the current distribution inside each filament can be considered as homogeneous.
The **skin depth** δ is defined as:

$$\delta = \frac{1}{\sqrt{\mu_0 \kappa_\Gamma \omega}} \tag{2}$$

The fundamental relation is:

$$\underline{\mathbf{u}}_\Lambda = \underline{\mathbf{Z}}_\Lambda \cdot \underline{\mathbf{i}}_\Lambda \tag{3}$$

where

- $\underline{\mathbf{u}}_\Lambda \in \mathbb{C}^n$ is the vector of filament voltages;
- $\underline{\mathbf{i}}_\Lambda \in \mathbb{C}^n$ is the vector of filament currents;
- $\underline{\mathbf{Z}}_\Lambda \in \mathbb{C}^{n \times n}$ is the matrix of filament impedances.

The filaments impedance matrix is defined as:

$$\underline{\mathbf{Z}}_{\Lambda} = \begin{bmatrix} Z_{11} & \cdots & Z_{1n} \\ \vdots & \ddots & \vdots \\ Z_{n1} & \cdots & Z_{nn} \end{bmatrix} = \begin{bmatrix} R_{11} + j\omega L_{11} & \cdots & j\omega L_{1n} \\ \vdots & \ddots & \vdots \\ j\omega L_{n1} & \cdots & R_{nn} + j\omega L_{nn} \end{bmatrix} \tag{4}$$

Defining $\mathbf{C} \in \mathbb{C}^{n \times K}$, the **connectivity matrix**, where K represents the number of conductors, we can relate the filaments' quantities, $\underline{\mathbf{i}}_\Lambda$ and $\underline{\mathbf{u}}_\Lambda$, to the terminal quantities $\underline{\mathbf{I}}$ and $\underline{\mathbf{U}}$ with the relationships:

$$\underline{\mathbf{I}} = \mathbf{C}^\top \cdot \underline{\mathbf{i}}_\Lambda \tag{5}$$

$$\underline{\mathbf{u}}_\Lambda = \mathbf{C} \cdot \underline{\mathbf{U}} \tag{6}$$

where $\top$ denotes the transpose of a matrix.

In a simple case of only one conductor, the connectivity matrix becomes $\mathbf{C} \in \mathbb{C}^{n \times 1}$ and by applying this to (5) and (6) we can write:

$$\underline{\mathbf{I}} = \mathbf{C}^{\top} \cdot \underline{\mathbf{i}}_{\Lambda} = \sum_{v=1}^{n} \underline{\mathbf{i}}_{\Lambda,v} \tag{7}$$

$$\underline{\mathbf{u}}_{\Lambda} = \mathbf{C} \cdot \underline{\mathbf{U}} \Rightarrow \underline{\mathbf{u}}_{\Lambda,1} = \underline{\mathbf{u}}_{\Lambda,2} = \cdots = \underline{\mathbf{u}}_{\Lambda,n} = \underline{\mathbf{U}} \tag{8}$$

- Terminal current is the **sum** of all filament currents;
- Filament voltages are all **equal** to the terminal voltage.

We can write the symmetric terminal impedance matrix, $\underline{\mathbf{Z}} \in \mathbb{C}^{K \times K}$, as:

$$\underline{\mathbf{Z}} = (\mathbf{C}^{\top} \cdot \underline{\mathbf{Z}}_{\Lambda}^{-1} \cdot \mathbf{C})^{-1} \tag{9}$$

By using the relationship $\underline{\mathbf{U}} = \underline{\mathbf{Z}} \cdot \underline{\mathbf{I}}$, (3), (6) and (9) we obtain:

$$\underline{\mathbf{i}}_{\Lambda} = \underline{\mathbf{Z}}_{\Lambda}^{-1} \cdot \mathbf{C} \cdot \underline{\mathbf{Z}} \cdot \underline{\mathbf{I}} \tag{10}$$

that is the expression of the filament currents in terms of the terminal current.

Stimulating the Conductor

Each conductor can be stimulated using two different methods:

1. **Terminal Current Stimulation**: the terminal current $\underline{\mathbf{I}}$ is given, and the current distribution $\underline{\mathbf{i}}_\Lambda$ is determined using the relationship:

$$\underline{\mathbf{i}}_\Lambda = \underline{\underline{\mathbf{Z}}}_\Lambda^{-1} \cdot \mathbf{C} \cdot \underline{\underline{\mathbf{Z}}} \cdot \underline{\mathbf{I}}, \tag{11}$$

   as shown in Eq. (10).

2. **Terminal Voltage Stimulation**: the terminal voltage $\underline{\mathbf{U}}$ is specified, and the current distribution $\underline{\mathbf{i}}_\Lambda$ is derived using the relationship:

$$\underline{\mathbf{i}}_\Lambda = \underline{\underline{\mathbf{Z}}}_\Lambda^{-1} \cdot \mathbf{C} \cdot \underline{\mathbf{U}}, \tag{12}$$

   derived from combining Eq. (3) and Eq. (6).

Stimulating the Conductor

In both methods, the current distribution $\underline{\mathbf{i}}_\Lambda$ over the filaments of the conductor is calculated, either from a known terminal current or a known terminal voltage.

Skin and proximity effects give rise to an inhomogeneous current distribution leading to an inhomogeneous losses component.
The resistance R_{vv} of each filament $v = 1, \ldots, n$ is given by:

$$R_{vv} = \frac{l_{\Lambda,v}}{\kappa_\Gamma \cdot A_{\Lambda,v}} \tag{13}$$

where $l_{\Lambda,v}$ is the filament's length in z-direction, and $A_{\Lambda,v} = t_\Lambda \cdot w_\Lambda$ its cross section area.

The losses P_l can be either calculated from the terminal quantities as:

$$P_l = \frac{\mathcal{R}(\underline{\mathbf{U}} \cdot \underline{\mathbf{I}}^*)}{2} = \frac{|\underline{\mathbf{I}}|^2 \cdot \mathcal{R}(\underline{\mathbf{Z}})}{2} \tag{14}$$

or by summing up the filaments losses:

$$P_l = \frac{\mathcal{R}(\underline{\mathbf{u}}_\Lambda^\top \cdot \underline{\mathbf{i}}_\Lambda^*)}{2} = \frac{\mathcal{R}(\underline{\mathbf{i}}_\Lambda^\top \cdot \underline{\mathbf{Z}}_\Lambda \cdot \underline{\mathbf{i}}_\Lambda^*)}{2} \tag{15}$$

Starting from (4), the filaments impedance matrix $\underline{\mathbf{Z}}_\Lambda$ can be written as:

$$\underline{\mathbf{Z}}_\Lambda = \mathbf{R}_\Lambda + j\omega\mathbf{L}_\Lambda \tag{16}$$

where $\mathbf{R}_\Lambda$ is the diagonal resistance matrix consisting of $R_{\Lambda,vv}$ according to (13), and $\mathbf{L}_\Lambda$ is the symmetric positive definite inductance matrix. It consists of self-inductances $L_{\Lambda,vv}$ on the matrix diagonal, and off-diagonal mutual inductances $L_{\Lambda,vm}$, $v \neq m = 1, \ldots, n$.

Two Methods for Calculating the Impedance Matrix

To compute the impedance matrix $\underline{\mathbf{Z}}_\Lambda$ of a rectangular conductor subdivided into filaments, we present two distinct approaches:

- **Method 1: Green's Function Approach** [1]
- **Method 2: Energy Storage Approach** [2]

Both methods will be applied separately to derive the impedance matrix $\underline{\mathbf{Z}}_\Lambda$.

First Method: Green's Function Approach

The first method for calculating the impedance matrix $\underline{\mathbf{Z}}_\Lambda$ is based on the **Green's Function Approach**:

- This method utilizes the Green's function for Poisson's equation to compute the self and mutual inductances between filaments.
- By solving Poisson's equation under specific boundary conditions, we derive a function that models the potential field due to a source.
- The computed Green's function is then employed to determine the impedance matrix $\underline{\mathbf{Z}}_\Lambda$ for the conductor.

The following slides will present the detailed derivation and steps involved in this method.

Dirichlet Green's Function for Poisson's Equation

Given Poisson's equation

$$\nabla^2 u = -f \tag{17}$$

a Dirichlet Green's function $G(x, x')$ in a three-dimensional domain D must satisfy:

- Harmonic in x everywhere except at x':

$$\nabla_x^2 G(x, x') = 0, \quad x \neq x'; \tag{18}$$

- Zero on the boundary:

$$G(x, x') = 0, \quad x \in \partial D; \tag{19}$$

- Locally behaves like $\delta(x - x')$:

$$G(x' + \epsilon, x') \sim -\frac{1}{4\pi|\epsilon|}, \quad |\epsilon| \to 0. \tag{20}$$

Globally, we can write:

$$G(x, x') = -\frac{1}{4\pi|x - x'|} + F(x, x'), \tag{21}$$

where F is harmonic in the first variable, ensuring the boundary conditions are satisfied.
Another way to express this is:

$$\nabla_x^2 G(x, x') = \delta(x - x'), \tag{22}$$

which directly relates the Green's function to the Dirac delta function.

Consider the Green's function $G(x;x')$ for Poisson's equation in n-dimensional space. Assuming spherical symmetry:

$$G(x,0) = G(|x|) = G(r), \quad r = |x|.$$

The Laplacian in n dimensions for a radially symmetric function $G(r)$ is:

$$\nabla^2 G(r) = \frac{1}{r^{n-1}} \frac{d}{dr}\left(r^{n-1}\frac{dG}{dr}\right). \tag{23}$$

Integrating over a sphere of radius R centered at the origin, we get:

$$1 = \int_{|x|<R} \nabla^2 G(r)\, dV. \tag{24}$$

Recap of the Divergence Theorem

The Divergence Theorem relates the flux of a vector field through a closed surface to the volume integral of its divergence:

$$\int_V (\nabla \cdot \mathbf{F})\, dV = \int_{\partial V} \mathbf{F} \cdot \mathbf{n}\, dS, \tag{25}$$

where V is the volume, ∂V its boundary, $\mathbf{F}$ the vector field, and $\mathbf{n}$ the outward unit normal vector.
Applied to the Green's function:

$$\int_{|x|<R} \nabla^2 G(r)\, dV = \int_{|x|=R} \frac{\partial G}{\partial r}(R)\, dS.$$

We apply the Divergence Theorem by considering the vector field:

$$\mathbf{F} = \nabla G(r).$$

The divergence of $\mathbf{F}$ is $\nabla \cdot \nabla G(r) = \nabla^2 G(r)$. Therefore:

$$\int_{|x|<R} \nabla^2 G(r)\, dV = \int_{|x|=R} \nabla G(r) \cdot \mathbf{n}\, dS = \int_{|x|=R} \frac{\partial G}{\partial r}(R)\, dS. \tag{26}$$

Here, $\frac{\partial G}{\partial r}(R)$ is the radial derivative of $G(r)$ at $r = R$, integrated over the sphere's surface.

The surface integral over the sphere $|x| = R$ becomes:

$$\int_{|x|=R} \frac{\partial G}{\partial r}(R)\, dS = S_{n-1} R^{n-1} G'(R), \tag{27}$$

where S_{n-1} is the surface area of the unit sphere in $(n-1)$ dimensions, and $G'(R) = \frac{\partial G}{\partial r}(R)$ is the radial derivative at R.
The factor $S_{n-1}R^{n-1}$ accounts for the surface area of a sphere in n-dimensions.

Combining (24) and (27), we find:

$$S_{n-1} R^{n-1} G'(R) = 1, \tag{28}$$

Rearranging and integrating with respect to R:

$$G'(R) = \frac{1}{S_{n-1} R^{n-1}}, \tag{29}$$

which upon integration gives:

$$G(R) = \int \frac{1}{S_{n-1} R^{n-1}} \, dR = -\frac{1}{(n-2) S_{n-1} R^{n-2}} + C. \tag{30}$$

To satisfy $G(r) \to 0$ as $r \to \infty$, we set $C = 0$, resulting in:

$$G(r) = -\frac{1}{(n-2) S_{n-1} r^{n-2}}. \tag{31}$$

1D Green's Function

For the one-dimensional case ($n = 1$), the Green's function satisfies:

$$\nabla^2 G(x, x') = \delta(x - x'), \tag{32}$$

leading to:

$$G(x, x') = \frac{1}{2}|x - x'|. \tag{33}$$

In 1D, the Green's function grows linearly with distance, reflecting the different behavior compared to higher dimensions.

Consider the zero set of the function:

$$x \mapsto -\frac{1}{|x-b|} + \frac{\lambda}{|x-c|}, \tag{34}$$

where $b \neq c$ and $\lambda > 0$. For a fixed x, the zero set is given by:

$$\frac{|x-c|}{|x-b|} = \lambda. \tag{35}$$

Lemma: If $\lambda \neq 1$, this represents a sphere. If $\lambda = 1$, it is a plane bisecting the line segment between b and c.

Squaring and rearranging, we get the sphere equation:

$$\lambda^2|x-b|^2 = |x-c|^2. \tag{36}$$

Expanding and rearranging leads to:

$$x = \frac{\lambda^2 b - c}{\lambda^2 - 1} + \frac{\lambda|c-b|}{|\lambda^2-1|}.$$

The center is at $\frac{\lambda^2 b-c}{\lambda^2-1}$ and radius $\frac{\lambda|c-b|}{|\lambda^2-1|}$, provided $\lambda \neq 1$.

In three dimensions ($n = 3$), to satisfy Laplace's equation:

$$\nabla^2 G(x, x') = \delta^3(x - x'), \tag{37}$$

with boundary conditions $G(x, x') = 0$ on the sphere's surface, use (34) with suitable values of b, c, and λ, and let the sphere have radius R.

- Choose $b = x'$ (source) and c outside the sphere.
- To make $G(x, x') = 0$ on the sphere's boundary, set $c = \lambda^2 x'$. This reduces (35) to:

$$|x| = \lambda|\lambda^2 x' - x'|/(\lambda^2 - 1) = \lambda|x'|. \tag{38}$$

  We get $\lambda = R/|x'|$.
- Scale by $1/4\pi$ for the correct form.

The Green's function for the three-dimensional case is:

$$G(x, x') = -\frac{1}{4\pi|x - x'|} + \frac{\lambda}{4\pi|x - \lambda^2 x'|}, \quad \lambda = \frac{R}{|x'|}. \tag{39}$$

2D Green's Function Strategy

In two dimensions ($n = 2$), the free Green's function behaves logarithmically. We construct a function that:

- Behaves like $|x - x'|$ near $x = x'$,
- Has no other zeros inside the circle,
- Equals 1 on the boundary $|x| = R$.

Taking the logarithm of this function ensures it satisfies the boundary conditions.

Repurposing (35) for two dimensions, we define:

$$\left\{ x \in \mathbb{R}^2 : \frac{\lambda |x - x'|}{|x - \lambda^2 x'|} = 1 \right\} \tag{40}$$

representing a circle of radius R with:

$$\lambda = \frac{R}{|x'|}. \tag{41}$$

The Green's function for the interior of a circle is:

$$G(x, x') = \frac{1}{2\pi} \log \left(\frac{\lambda |x - x'|}{|x - \lambda^2 x'|} \right), \tag{42}$$

where $\lambda = \frac{R}{|x'|}$. This ensures the correct logarithmic singularity at $x = x'$ and regularity elsewhere in the circle.

Verifying 2D Green's Function

Verifications for the Green's function:

- It behaves logarithmically near $x = x'$, appropriate for 2D.
- No other zeros inside the circle.
- It is zero on the boundary $|x| = R$.

Thus, $G(x, x')$ is a valid Green's function for a 2D circle.

Now that we have derived the equations arising from the solution of the 2-D Laplacian of the Dirichlet problem, we can proceed with the calculation of the self and mutual inductances between elements in the domain.

Given (42), we introduce the normalized coordinates as:

$$\xi := \frac{x}{R}, \qquad \xi' := \frac{x'}{R} \tag{43}$$

Rewriting (42) by eliminating λ for a stable numerical implementation, we have:

$$G(\xi, \xi') = -\frac{\mu_0 I}{2\pi}\left(\ln|\xi - \xi'| - \frac{1}{2}\ln\left(|\xi|^2|\xi'|^2 - 2\xi\cdot\xi' + 1\right)\right) \tag{44}$$

Using (44), the mutual inductance between two filaments can be calculated as:

$$L_{\Lambda,vm} = \frac{G(\xi, \xi') \cdot l_v}{I} \tag{45}$$

where ξ and ξ' denote coordinate vectors of the center of the two filaments v and m normalized to R in accordance to (43), and l_v is the length of the filament v, being identical for all filaments.

As long as the rectangular filaments' cross section aspect ratio corresponds to:

$$\frac{a_\Lambda}{b_\Lambda} \approx 1 \tag{46}$$

we can use **equivalent filaments** with equal cross section area with the corresponding radius:

$$\tilde{r}_\Lambda = \sqrt{\frac{a_\Lambda \cdot b_\Lambda}{\pi}} \tag{47}$$

for calculating filaments' self-inductances.

From (47) we can obtain the normalized cross section radius:

$$\rho = \frac{\tilde{r}_\Lambda}{R} \tag{48}$$

using (43).
Now, the self-inductance can be calculate as:

$$L_{\Lambda,vv} = -\frac{\mu_0 l_v}{2\pi}\left(\ln\rho - \frac{1}{2}\ln\left(\left(1-|\xi'|^2\right)^2 + \left(|\xi'|\rho\right)^2\right)\right) \tag{49}$$

where l_v denotes the length of the filaments.

The second method for calculating the impedance matrix $\underline{\mathbf{Z}}_\Lambda$ is the **Energy Storage Approach**:

- This method relies on the calculation of energy stored in the magnetic field generated by the current-carrying filaments.
- It involves the computation of self and mutual partial inductances using the magnetic vector potential.
- The energy expressions are utilized to derive the inductance matrix components, which are then used to construct the impedance matrix $\underline{\mathbf{Z}}_\Lambda$.

The subsequent slides will provide a comprehensive derivation of this method.

The formulation for computing self and partial inductances of rectangular filaments is in terms of **energy stored** in the magnetic field.
The energy stored can be expressed as:

$$W_M = \frac{1}{2} \int_{\substack{\text{throughout} \\ \text{the volume} \\ \text{containing} \\ \text{the current}}} \mathbf{A} \cdot \mathbf{J} \, dv \tag{50}$$

where dv is the infinitesimal volume element and $\mathbf{A}$ is the magnetic vector potential such that

$$\mathbf{B} = \nabla \times \mathbf{A} \tag{51}$$

Considering two rectangular filaments Λ_1 and Λ_2, each one carrying a total current $\underline{\mathbf{I}}_1$ and $\underline{\mathbf{I}}_2$, respectively.
The total magnetic field $\mathbf{A}$ can be defined as:

$$\mathbf{A} = \mathbf{A}_1 + \mathbf{A}_2 \tag{52}$$

where $\mathbf{A}_1$ is due to current $\underline{\mathbf{I}}_1$ and $\mathbf{A}_2$ is due to current $\underline{\mathbf{I}}_2$.
Given $\mathbf{A}$, the total magnetic energy surrounding Λ_1 and Λ_2 is :

$$W_M = \frac{1}{2}\int_{v_1} \mathbf{A}\cdot\mathbf{J}_1 dv_1 + \frac{1}{2}\int_{v_2} \mathbf{A}\cdot\mathbf{J}_2 dv_2 \tag{53}$$

where v_1 and v_2 are the volumes of the respective lands that enclose the respective current densities, $\mathbf{J}_1$ and $\mathbf{J}_2$.

Substituting $\mathbf{A} = \mathbf{A}_1 + \mathbf{A}_2$ into the total magnetic energy expression, we obtain:

$$W_M = \frac{1}{2}\int_{v_1} \mathbf{A}_1 \cdot \mathbf{J}_1 \, dv_1 + \frac{1}{2}\int_{v_2} \mathbf{A}_1 \cdot \mathbf{J}_2 \, dv_2 + \frac{1}{2}\int_{v_2} \mathbf{A}_2 \cdot \mathbf{J}_2 \, dv_2 + \frac{1}{2}\int_{v_1} \mathbf{A}_2 \cdot \mathbf{J}_1 \, dv_1 \tag{54}$$

The total magnetic energy in the field is represented in terms of self and mutual partial inductances of the two filaments as:

$$W_M = \frac{1}{2}L_{p1}I_1^2 + \frac{1}{2}M_{p12}I_1I_2 + \frac{1}{2}L_{p2}I_2^2 + \frac{1}{2}M_{p21}I_2I_1 \tag{55}$$

where mutual partial inductances are reciprocal (i.e., $M_{p12} = M_{p21}$).

Comparing (54) and (55) the various self and mutual partial inductances can be found from:

$$L_{p1} = \frac{1}{I_1^2} \int_{v_1} \mathbf{A}_1 \cdot \mathbf{J}_1 \, dv_1 \tag{56a}$$

$$L_{p2} = \frac{1}{I_2^2} \int_{v_2} \mathbf{A}_2 \cdot \mathbf{J}_2 \, dv_2 \tag{56b}$$

$$M_{p12} = \frac{1}{I_1 I_2} \int_{v_2} \mathbf{A}_1 \cdot \mathbf{J}_2 \, dv_2 \tag{56c}$$

$$M_{p21} = \frac{1}{I_1 I_2} \int_{v_1} \mathbf{A}_2 \cdot \mathbf{J}_1 \, dv_1 \tag{56d}$$

The equation for the vector magnetic potential given by:

$$\mathbf{A} = \frac{\mu_0}{4\pi} \int_v \frac{\mathbf{J}\, dv}{R} \tag{57}$$

represents the vector magnetic potential $\mathbf{A}$ at a point due to a current distribution $\mathbf{J}$ over a volume v, where R is the distance between the current element and the point at which $\mathbf{A}$ is being calculated.

Substituting (57) into (56) gives:

$$L_{p1} = \frac{1}{I_1^2} \int_{v_1} \int_{v_1'} \frac{\mu_0}{4\pi} \frac{\mathbf{J}_1 \cdot \mathbf{J}_1' \, dv_1' \, dv_1}{R} \tag{58a}$$

$$L_{p2} = \frac{1}{I_2^2} \int_{v_2} \int_{v_2'} \frac{\mu_0}{4\pi} \frac{\mathbf{J}_2 \cdot \mathbf{J}_2' \, dv_2' \, dv_2}{R} \tag{58b}$$

$$M_{p12} = \frac{1}{I_1 I_2} \int_{v_2} \int_{v_2'} \frac{\mu_0}{4\pi} \frac{\mathbf{J}_1 \cdot \mathbf{J}_2' \, dv_2' \, dv_2}{R} \tag{58c}$$

$$M_{p21} = \frac{1}{I_1 I_2} \int_{v_1} \int_{v_1'} \frac{\mu_0}{4\pi} \frac{\mathbf{J}_2 \cdot \mathbf{J}_1' \, dv_1' \, dv_1}{R} \tag{58d}$$

where the term R is the distance between two differential chunks of current $\mathbf{J}_i \, dv_i$ and $\mathbf{J}_j' \, dv_j'$.

Two assumptions to make (58) practically useful for the computation:

- the currents I with density $\mathbf{J}$ in volume v are uniformly distributed over the cross sections of the rectangular filaments;
- the currents densities $\mathbf{J}$ in v are uniformly distributed along the length of filaments.

Hence, we can write:

$$Jdv = \frac{I}{A} dAdl \tag{59}$$

The self partial inductances are then computed from:

$$L_p = \frac{1}{AA'} \int_A \int_{A'} M_f \, dA' \, dA \tag{60}$$

where A and A' are over the same filament, and M_f is the Neumann integral denoting the mutual partial inductance between two filamentary currents (within the same element) that are separated by distance R:

$$M_f = \frac{\mu_0}{4\pi} \int_l \int_{l'} \frac{dl' \cdot dl}{R} \tag{61}$$

In the case of two different filaments, the mutual partial inductance between them is obtained from:

$$M_p = \frac{1}{AA'} \int_A \int_{A'} M_f \, dA' \, dA \tag{62}$$

where A and A' are over different filaments.

The computation of the self and mutual partial inductances involves **representing the currents of each rectangular element as being composed of filaments**. We obtain the total self and mutual partial inductances of the lands as the **summation**, over the cross-sectional areas of the filaments, of these mutual partial inductances between the filaments.

The mutual partial inductance between two filaments of lengths l and m, whose endpoints are offset by s and separated by a distance d, can be expressed as:

$$\begin{aligned} M_f &= \frac{\mu_0}{4\pi} \left[f(z) \right] \Big|_{(s+m),(l+s)}^{(l+s+m),s} (z) \\ &= \frac{\mu_0}{4\pi} \left[f(l+s+m) - f(s+m) + f(s) - f(l+s) \right] \end{aligned} \tag{63}$$

where

$$f(z) = z \ln \left(z + \sqrt{z^2 + d^2} \right) - \sqrt{z^2 + d^2} \tag{64}$$

With two filaments of identical length l and their endpoints coinciding, giving $m = l$ and $s = -l$, (63) reduces to:

$$\begin{aligned} M_f &= \frac{\mu_0}{4\pi} \left[f(z) \right] \Big|_{0,0}^{l,-l} \\ &= \frac{\mu_0}{4\pi} \left[f(l) - f(0) + f(-l) - f(0) \right] \\ &= \frac{\mu_0}{4\pi} \left[l \ln \left(l + \sqrt{l^2 + d^2} \right) - l \ln \left(-l + \sqrt{l^2 + d^2} \right) - 2\sqrt{l^2 + d^2} + 2d \right] \\ &= \frac{\mu_0}{2\pi} \left(l \sinh^{-1} \frac{l}{d} - \sqrt{l^2 + d^2} + d \right) \end{aligned} \tag{65}$$

First, the case of a **zero thickness** rectangular filaments is considered:

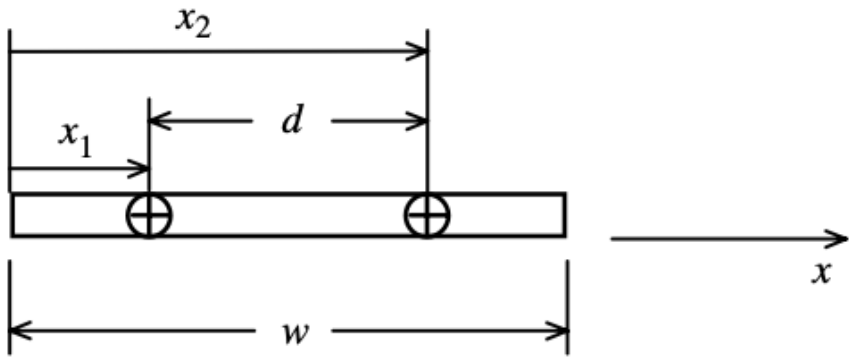

Figure 3: Self partial inductance for a land of zero thickness ($t = 0$).

As illustrated in Fig. 3, the self partial inductance, $L_{p(t=0)}$, can be calculate integrating (60) over the same cross-section filament obtaining:

$$L_{p(t=0)} = \frac{\mu_0}{4\pi}\frac{1}{w^2}\int_{x2=0}^{w}\int_{x1=0}^{w} M_f \; dx_1 dx_2 \tag{66}$$

where the distance d between two filaments is calculated as $d = \sqrt{(x_2 - x_1)^2}$.

Performing the integration of (66), gives:

$$L_{p(t=0)} = \frac{\mu_0}{2\pi}\frac{1}{w^2}\left[lw^2 \ln\left(\frac{l}{w} + \sqrt{\left(\frac{l}{w}\right)^2 + 1}\right) + l^2 w \ln\left(\frac{w}{l} + \sqrt{\left(\frac{w}{l}\right)^2 + 1}\right) + \frac{1}{3}\left(l^3 + w^3\right) - \frac{1}{3}\left(l^2 + w^2\right)^{3/2}\right] \tag{67}$$

where $t = 0$.

Equation (67) can be rewritten in terms of the "aspect ratio" of the rectangular filament as the ratio of the land length to land width, $u = l/w$, obtaining:

$$\frac{L_{p(t=0)}}{l} = \frac{\mu_0}{2\pi}\left[\ln\left(u+\sqrt{u^2+1}\right) + u\ln\left(\frac{1}{u}+\sqrt{\left(\frac{1}{u}\right)^2+1}\right) + \frac{1}{3}\left(u^2+\frac{1}{u}-\frac{\left(u^2+1\right)^{3/2}}{u}\right)\right] \tag{68}$$

where $u = l/w$ and $t = 0$.

For extreme values of the "aspect ratio" of the filaments, equation (68) can be approximated as:

$$\frac{L_{p(t=0)}}{l} \approx \frac{\mu_0}{2\pi} \begin{cases} \ln 2u + \frac{1}{2} + \frac{1}{3u} & u \gg 1,\ l \gg w \\ u\left(\ln \frac{2}{u} + \frac{1}{2} + \frac{u}{3}\right) & u \ll 1,\ l \ll w \end{cases} \tag{69}$$

where the $u \gg 1$ represents very long filaments and $u \ll 1$ represents very wide filaments.

Now the computation of the self partial inductance of a non-zero thickness filament is presented:

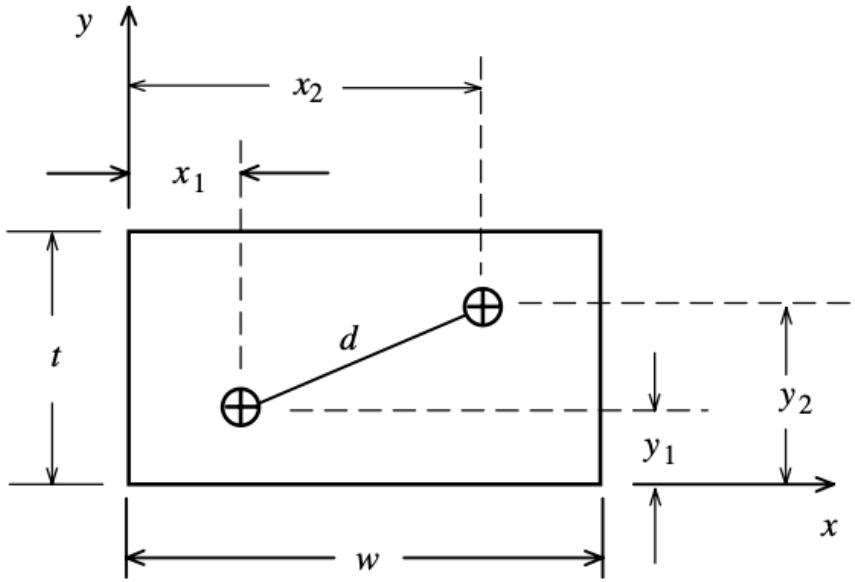

Figure 4: Self partial inductance for a land of non-zero thickness.

In the case of non-zero thickness land, described in Fig. 4, the self partial inductance L_p is calculated as:

$$L_p = \frac{1}{w^2 t^2} \int_{y2=0}^{t} \int_{y1=0}^{t} \int_{x2=0}^{w} \int_{x1=0}^{w} M_f \; dx_1 dx_2 dy_1 dy_2 \tag{70}$$

the distance d is now calculated as $d = \sqrt{(x_2 - x_1)^2 + (y_2 - y_1)^2}$

Hoer and Love give that result as:

$$L_p = \frac{\mu_0}{4\pi}\frac{1}{t^2 w^2}\left[\left[\left[f(x,y,z)\right]\overset{w}{\underset{0}{(\mathrm{x})}}\right]\overset{t}{\underset{0}{(\mathrm{y})}}\right]\overset{l}{\underset{0}{(\mathrm{z})}} \tag{71}$$

where:

$$\left[\left[\left[f(x,y,z)\right]\overset{q_1}{\underset{q_2}{(\mathrm{x})}}\right]\overset{r_1}{\underset{r_2}{(\mathrm{y})}}\right]\overset{s_1}{\underset{s_2}{(\mathrm{z})}} = \sum_{i=1}^{2}\sum_{j=1}^{2}\sum_{k=1}^{2}(-1)^{i+j+k+1}\ f(q_i, r_j, s_k) \tag{72}$$

$$
\begin{aligned}
f(x,y,z) = & \left(\frac{y^2z^2}{4} - \frac{y^4}{24} - \frac{z^4}{24}\right) x \ln\left(x + \sqrt{x^2+y^2+z^2}\right) \\
& + \left(\frac{x^2z^2}{4} - \frac{x^4}{24} - \frac{z^4}{24}\right) y \ln\left(y + \sqrt{y^2+x^2+z^2}\right) \\
& + \left(\frac{x^2y^2}{4} - \frac{x^4}{24} - \frac{y^4}{24}\right) z \ln\left(z + \sqrt{z^2+x^2+y^2}\right) \\
& + \frac{1}{60}\left(x^4+y^4+z^4-3x^2y^2-3y^2z^2-3z^2x^2\right)\sqrt{x^2+y^2+z^2} \\
& - \frac{xyz^3}{6}\tan^{-1}\left(\frac{xy}{z\sqrt{x^2+y^2+z^2}}\right) - \frac{xy^3z}{6}\tan^{-1}\left(\frac{xz}{y\sqrt{x^2+y^2+z^2}}\right) \\
& - \frac{x^3yz}{6}\tan^{-1}\left(\frac{yz}{x\sqrt{x^2+y^2+z^2}}\right)
\end{aligned}
\tag{73}
$$

Non-Zero Thickness Rectangular Filaments

A more stable and simple formulation is introduced by Ruehli, expressing the self partial inductance, L_p only in terms of "aspect ratio" defining $u = l/w$ and $v = t/w$, obtaining:

$$\frac{L_p}{l} = \frac{2\mu_0}{\pi}\left\{\frac{\omega^2}{24u}\left[\ln\left(\frac{1+A_2}{\omega}\right) - A_5\right] + \frac{1}{24u\omega}\left[\ln(\omega + A_2) - A_6\right] + \frac{\omega^2}{60u}(A_4 - A_3)\right.$$
$$+ \frac{\omega^2}{24}\left[\ln\left(\frac{u+A_3}{\omega}\right) - A_7\right] + \frac{\omega^2}{60u}(\omega - A_2) + \frac{1}{20u}(A_2 - A_4) + \frac{u}{4\omega}A_5$$
$$- \frac{u^2}{6\omega}\tan^{-1}\left(\frac{\omega}{uA_4}\right) + \frac{u}{4\omega}A_6 - \frac{\omega}{6}\tan^{-1}\left(\frac{u}{\omega A_4}\right) + \frac{A_7}{4} - \frac{1}{6\omega}\tan^{-1}\left(\frac{u\omega}{A_4}\right)$$
$$+ \frac{1}{24\omega^2}\left[\ln(u + A_1) - A_7\right] + \frac{u}{20\omega^2}(A_1 - A_4) + \frac{1}{60\omega^2 u}(1 - A_2)$$
$$+ \frac{1}{60u\omega^2}(A_4 - A_1) + \frac{u}{20}(A_3 - A_4) + \frac{u^3}{24\omega^2}\left[\ln\left(\frac{1+A_1}{u}\right) - A_5\right]$$
$$\left. + \frac{u^3}{24\omega}\left[\ln\left(\frac{\omega + A_3}{u}\right) - A_6\right] + \frac{u^3}{60\omega^2}\left[(A_4 - A_1) + (u - A_3)\right]\right\} \tag{74}$$

where:

$$A_1 = (1 + u^2)^{1/2}$$

$$A_2 = (1 + \omega^2)^{1/2}$$

$$A_3 = (\omega^2 + u^2)^{1/2}$$

$$A_4 = (1 + \omega^2 + u^2)^{1/2}$$

$$A_5 = \ln\left(\frac{1 + A_4}{A_3}\right)$$

$$A_6 = \ln\left(\frac{\omega + A_4}{A_1}\right)$$

$$A_7 = \ln\left(\frac{u + A_4}{A_2}\right)$$

The mutual partial inductances between rectangular filaments is approximated as being between filaments at the centers of the filaments given by:

$$M_{p_{i,j}} = \frac{\mu_0}{2\pi} l \left[\ln\left(\frac{l}{d_{i,j}} + \sqrt{\left(\frac{l}{d_{i,j}}\right)^2 + 1} \right) - \sqrt{1 + \left(\frac{d_{i,j}}{l}\right)^2} + \frac{d_{i,j}}{l} \right] \quad (75)$$

where $d_{i,j}$ is the distance between the centers of filaments i and j.

Exercise

Exercise Overview

In this exercise, we will analyze the behavior of a rectangular conductor under different frequencies. The simulations will involve calculating the losses and errors when the conductor is stimulated by either setting a terminal current or a terminal voltage.

The following properties are used for the rectangular conductor:

- **Width** (w): 3.81×10^{-4} m
- **Thickness** (t): 3.556×10^{-5} m
- **Length** (l): 1 m
- **Material**: Copper (Resistivity, $\rho = 1/(5.889 \times 10^7)\ \Omega \cdot m$)

Frequency Range Studied:

- Frequencies are studied in a logarithmic scale from 1 Hz to 1×10^9 Hz.
- There are 5 frequency steps per decade.

Method 1 - Non-Uniform Mesh

- **Description**: The mesh is generated using a sine function, resulting in a lower density of grid points near the center and higher density near the edges. This approach provides finer resolution where the current density is expected to be higher.
- **Mesh Generation**:
  - Function: `generateNonUniformMesh(width, height, numPointsX, numPointsY)`
  - Non-uniform grid points are created using a sinusoidal distribution:

$$\text{grid} = \text{minVal} + (\text{maxVal} - \text{minVal}) \cdot \frac{\sin(t - \pi/2) + 1}{2}$$

  - **Mesh Configurations**:
    - $nx = ny = 40$
    - $nx = ny = 50$
    - $nx = ny = 60$

Method 2 - Uniform Mesh

- **Description**: The grid points are evenly spaced along both width and height, but with different numbers of points ($nx \neq ny$). Future work: use a non-uniform mesh.
- **Mesh Generation**:
  - Function: `generateUniformMesh(width, height, nx, ny)`
  - Uniform grid points are created using linearly spaced values:

$$x = \text{linspace}(0, \text{width}, nx), \quad y = \text{linspace}(0, \text{height}, ny)$$

  - **Mesh Configurations**:
    - $nx = 43$, $ny = 4$
    - $nx = 86$, $ny = 8$
    - $nx = 172$, $ny = 16$

Legend for Current Stimulation Results

- - - - - Reference Losses

——— Method 1 Direct (Config 1, nx=40, ny=40)

——— Method 1 Direct (Config 2, nx=50, ny=50)

——— Method 1 Direct (Config 3, nx=60, ny=60)

——— Method 2 Direct (Config 1, nx=43, ny=4)

——— Method 2 Direct (Config 2, nx=86, ny=8)

——— Method 2 Direct (Config 3, nx=172, ny=16)

Method 1 Summary Losses Errors Percentage Linear

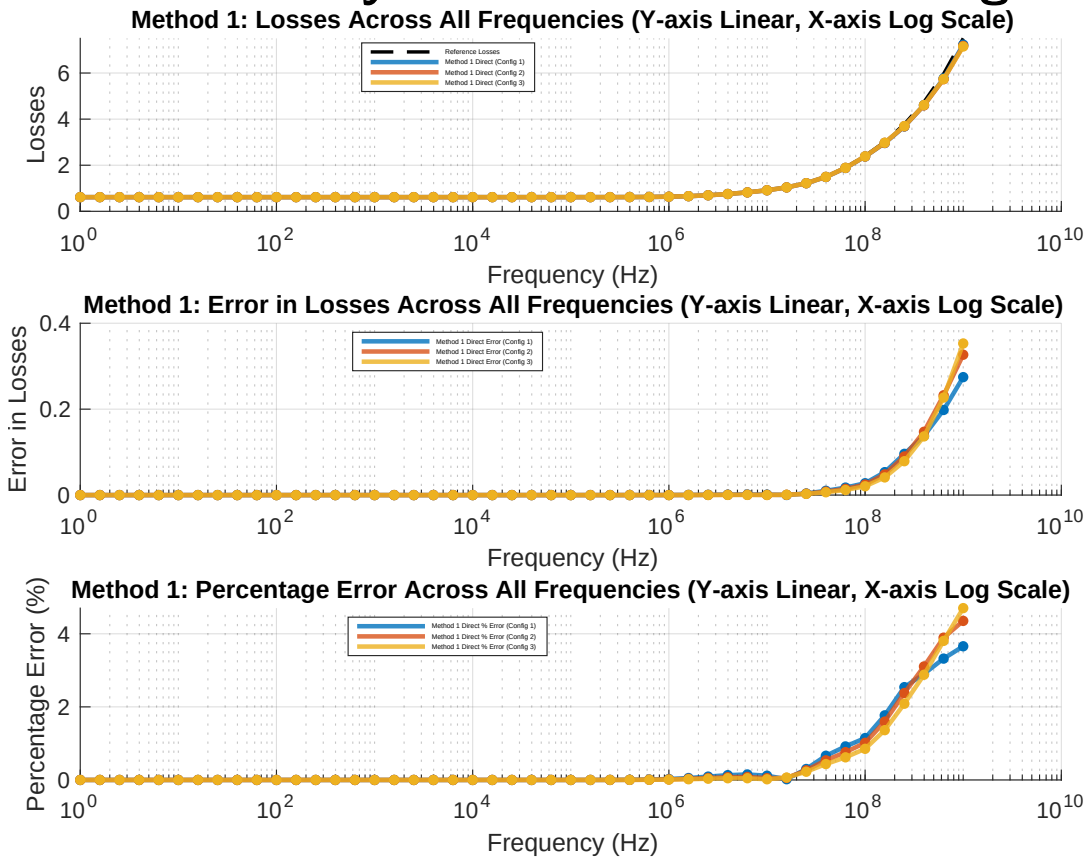

Method 1 Summary Losses Errors Percentage LogLog

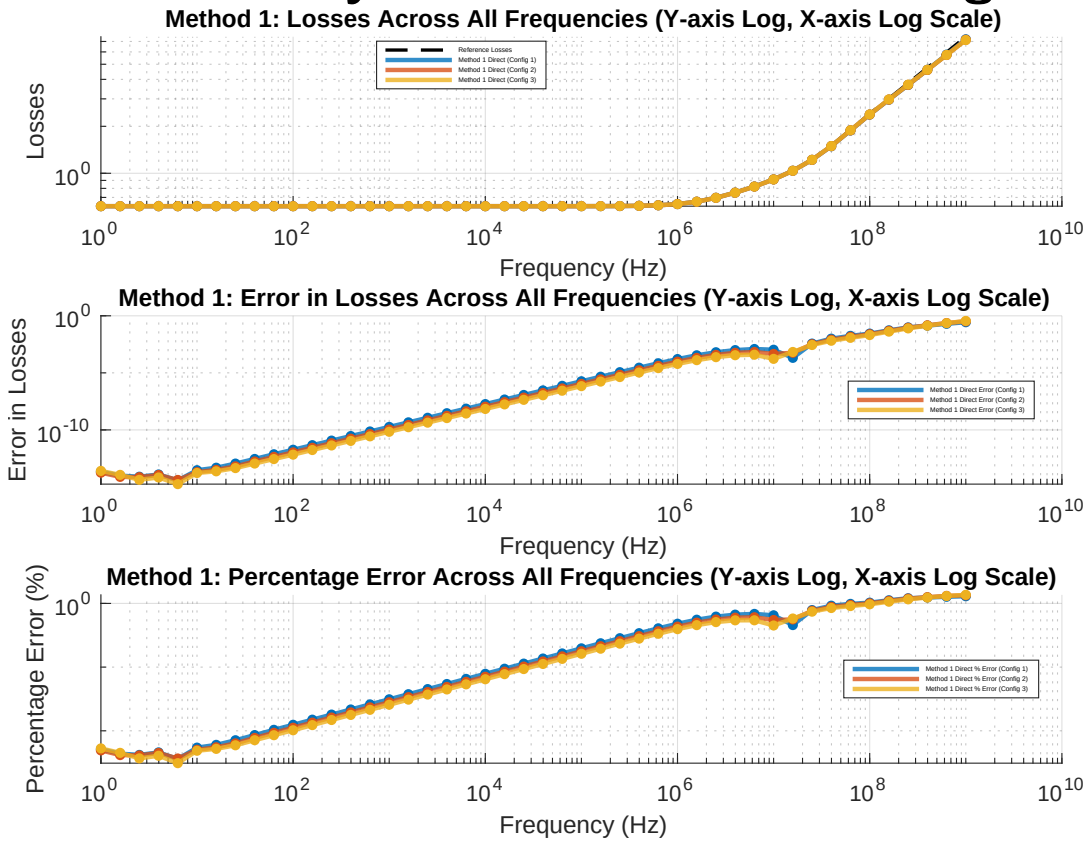

Method 2 Summary Losses Errors Percentage Linear

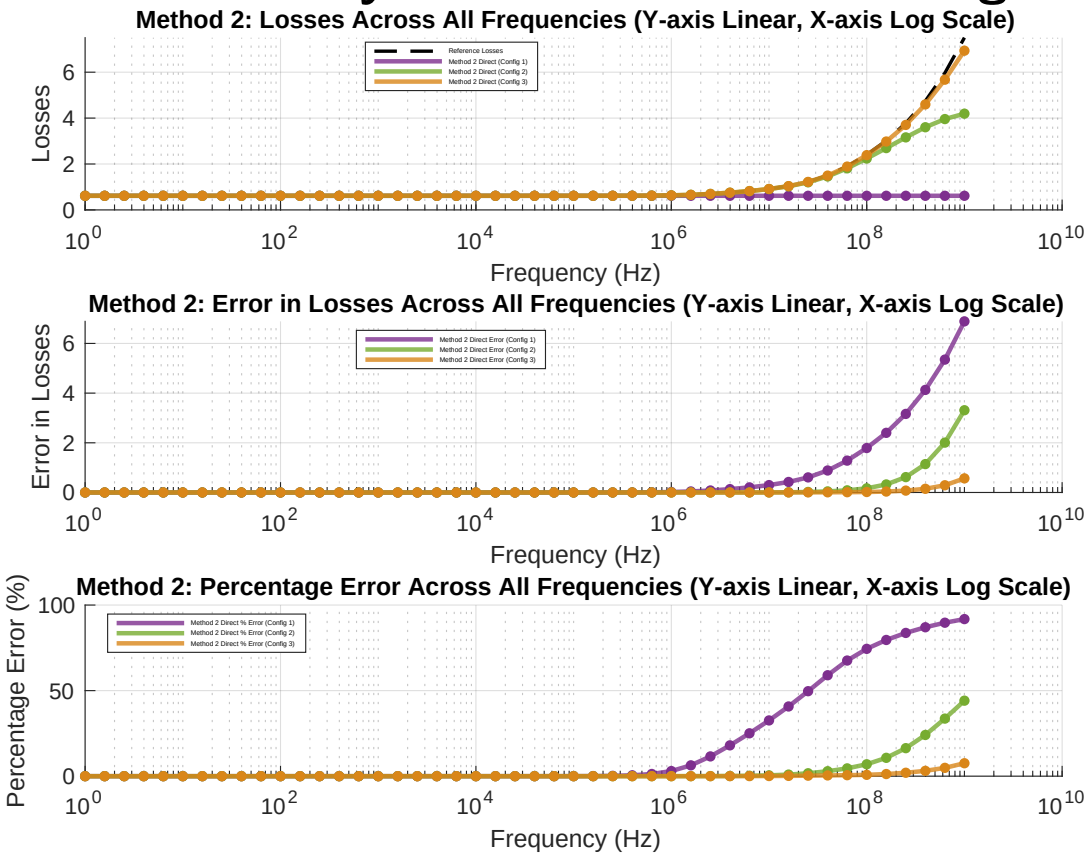

Method 2 Summary Losses Errors Percentage LogLog

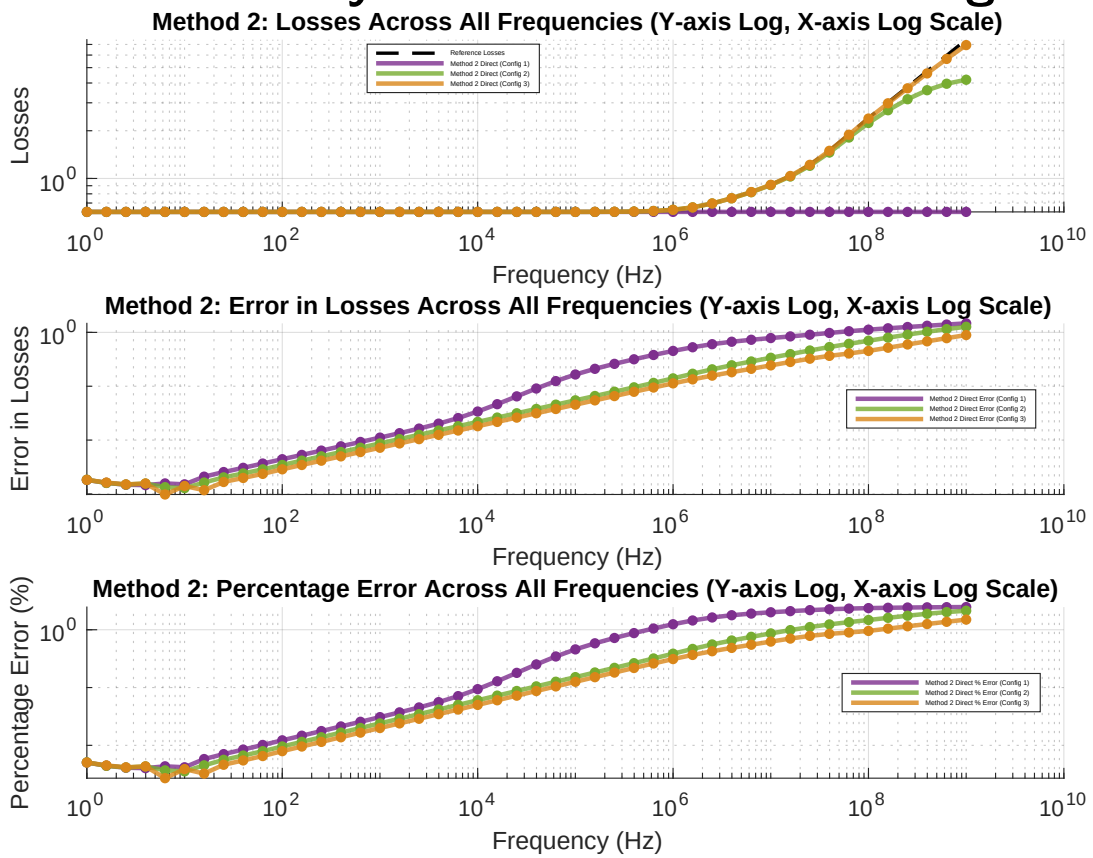

Method 1 and 2 Summary Losses Errors Percentage Linear

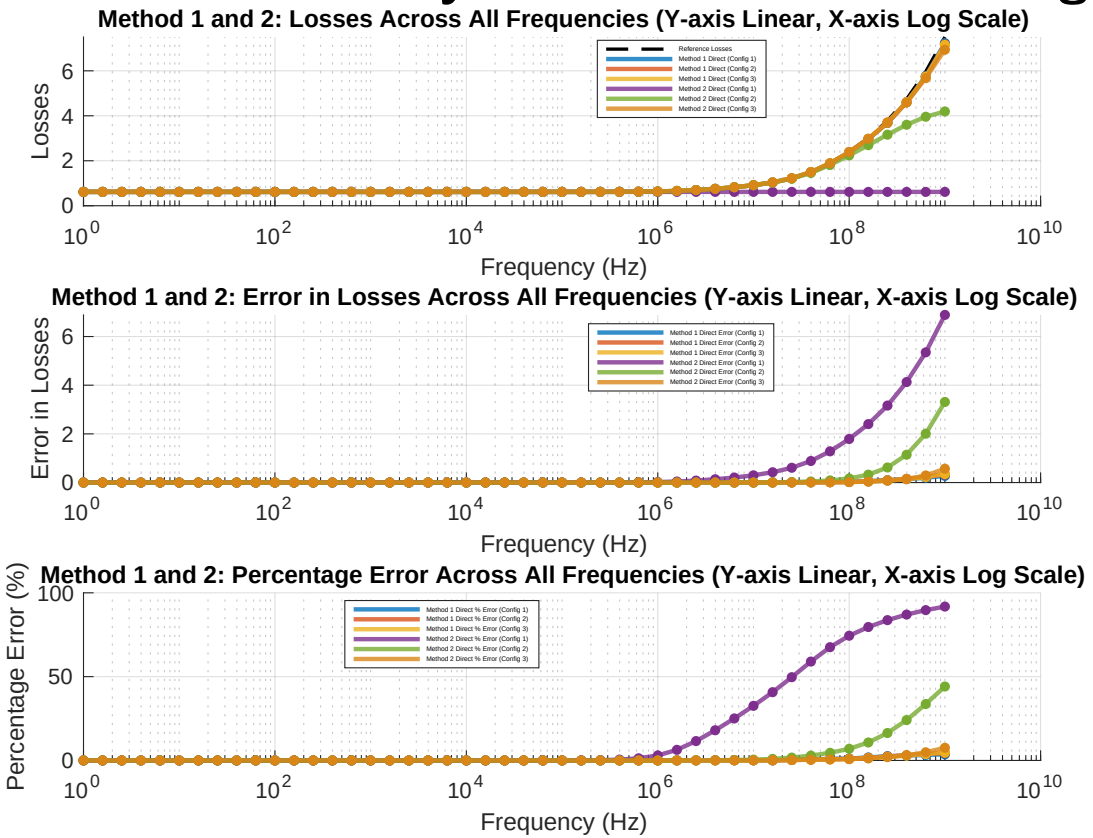

Method 1 and 2 Summary Losses Errors Percentage LogLog

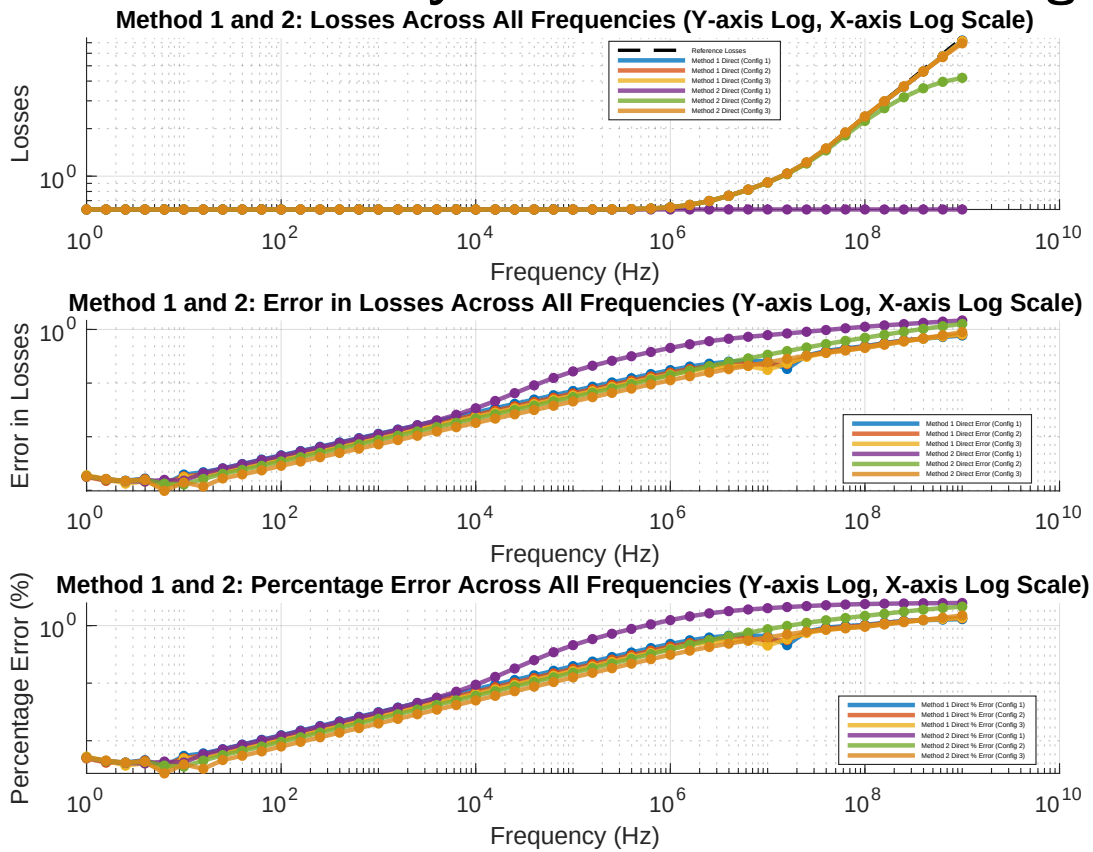

Combined Analysis of Method 1 and Method 2:

- Both methods exhibit an increasing trend in errors with higher frequencies, with significant differences becoming evident beyond 10^6 Hz.
- **Mesh Refinement:** Increasing the mesh density (larger nx, ny) reduces errors for both methods, indicating the importance of a finer mesh for improved accuracy.
- **Performance Comparison:**
  - At higher frequencies, Method 2 demonstrates superior performance with lower errors, suggesting its effectiveness in handling high-frequency scenarios.
  - For both methods, further convergence studies with much finer meshes are recommended to ensure accurate results. This will require substantial computational resources.

Legend: Voltage Stimulation

Legend for Voltage Stimulation Results

- - - - - Reference Losses

——— Method 1 Direct (Config 1, nx=40, ny=40)

——— Method 1 Direct (Config 2, nx=50, ny=50)

——— Method 1 Direct (Config 3, nx=60, ny=60)

——— Method 2 Direct (Config 1, nx=43, ny=4)

——— Method 2 Direct (Config 2, nx=86, ny=8)

——— Method 2 Direct (Config 3, nx=172, ny=16)

Method 1 Summary Losses Errors Percentage Linear

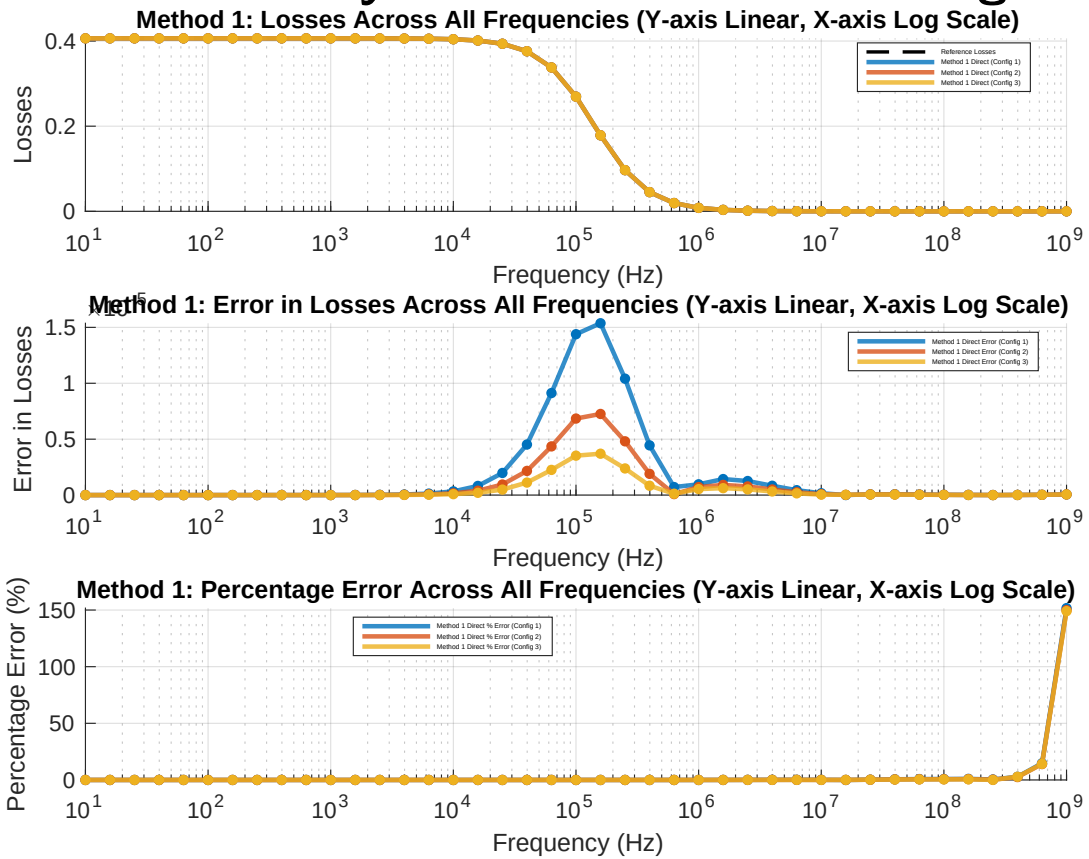

Method 1 Summary Losses Errors Percentage LogLog

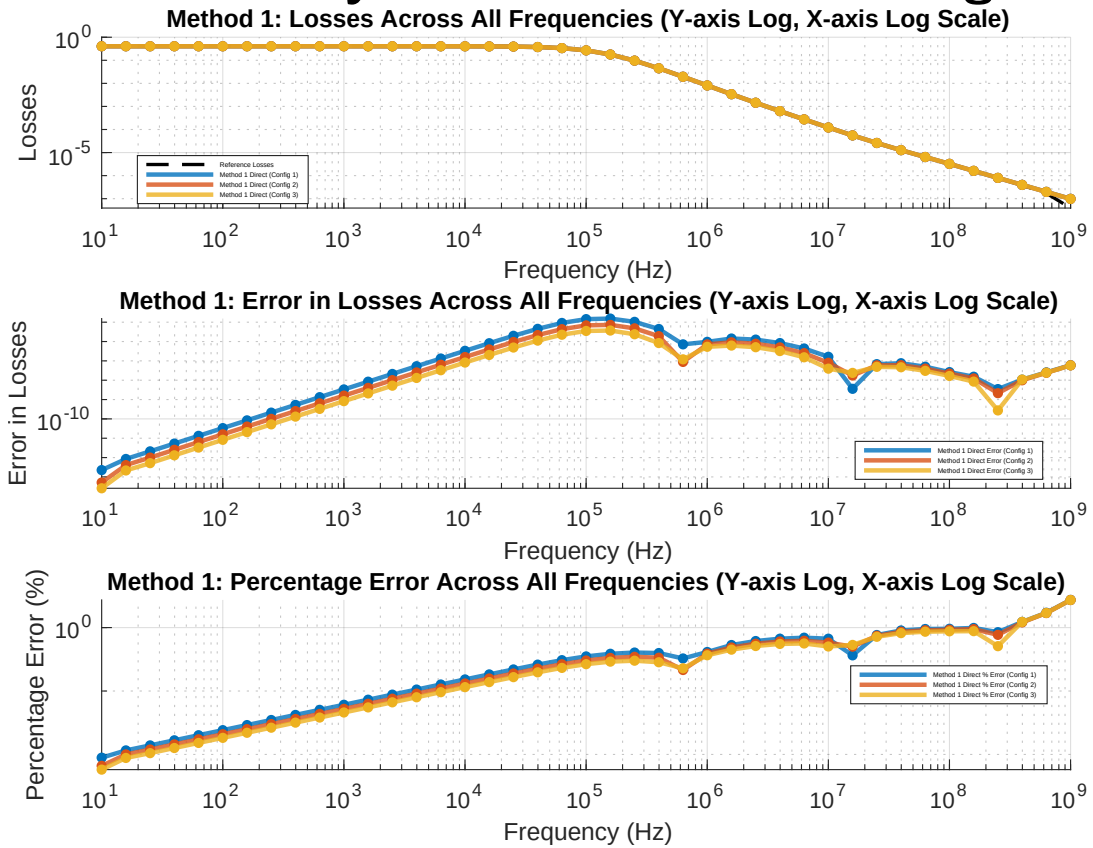

Method 2 Summary Losses Errors Percentage Linear

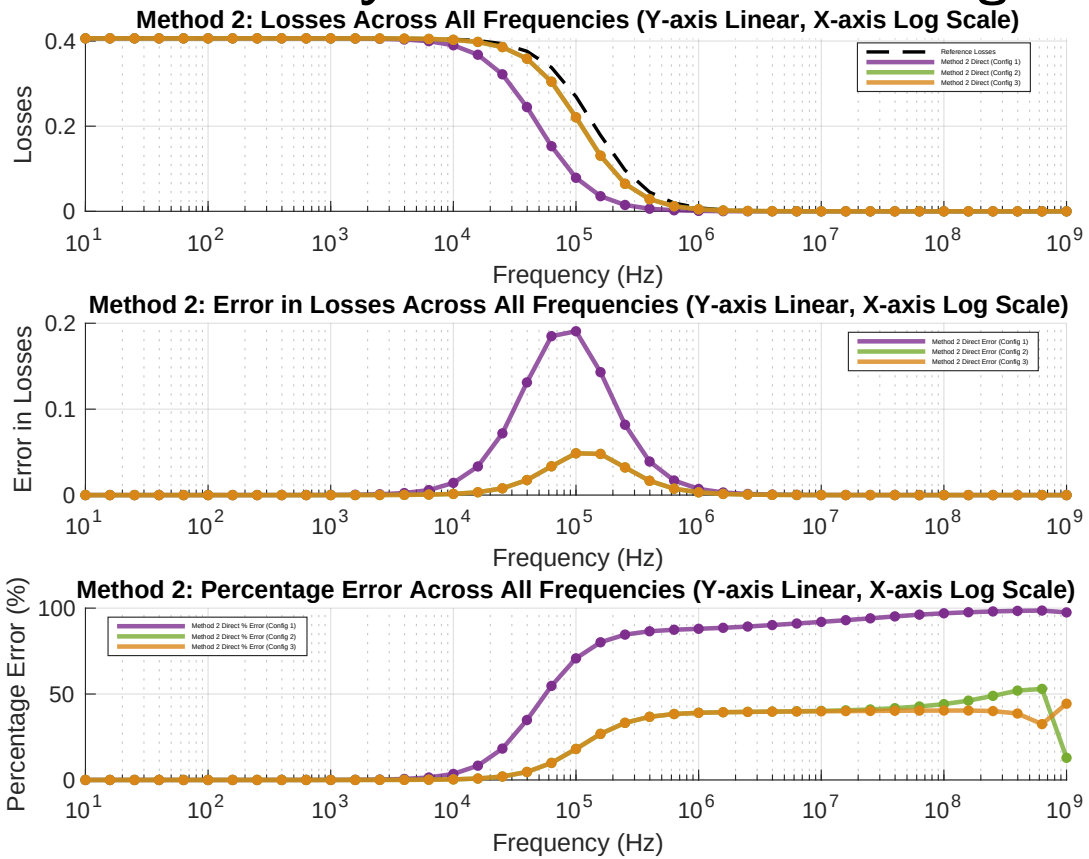

Method 2 Summary Losses Errors Percentage LogLog

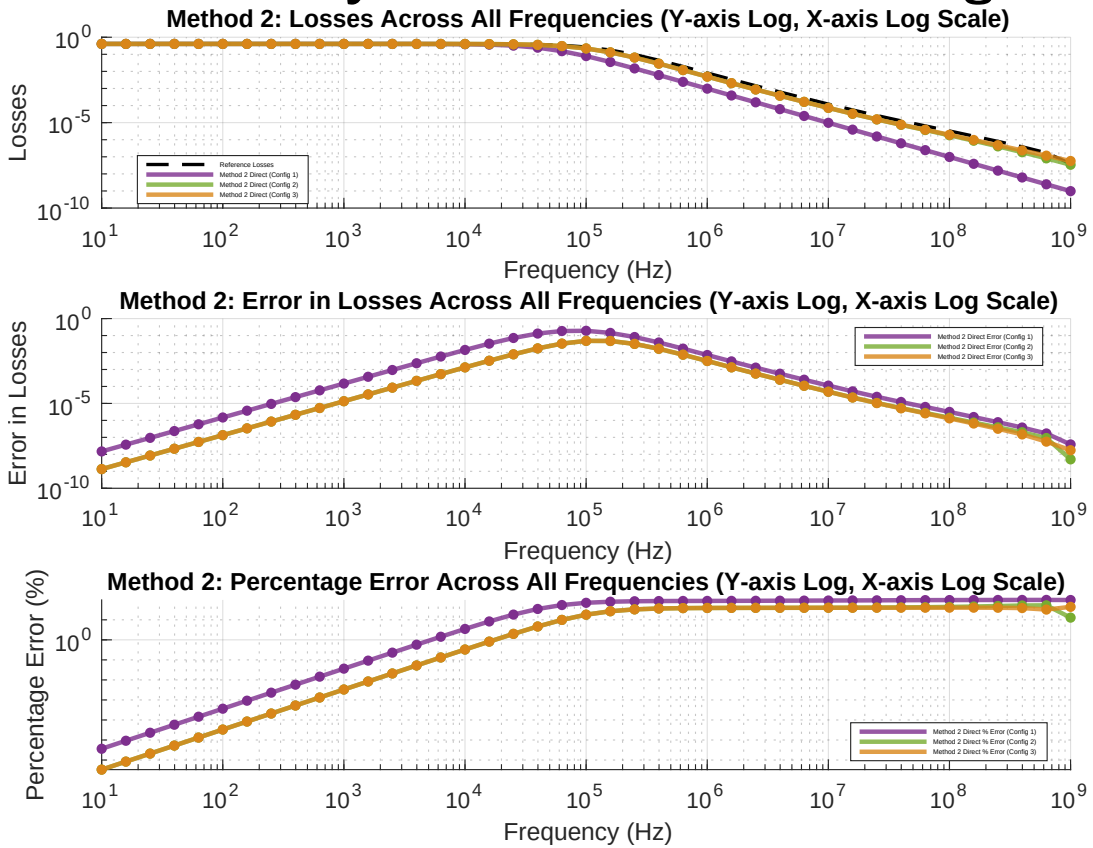

Method 1 and 2 Summary Losses Errors Percentage Linear

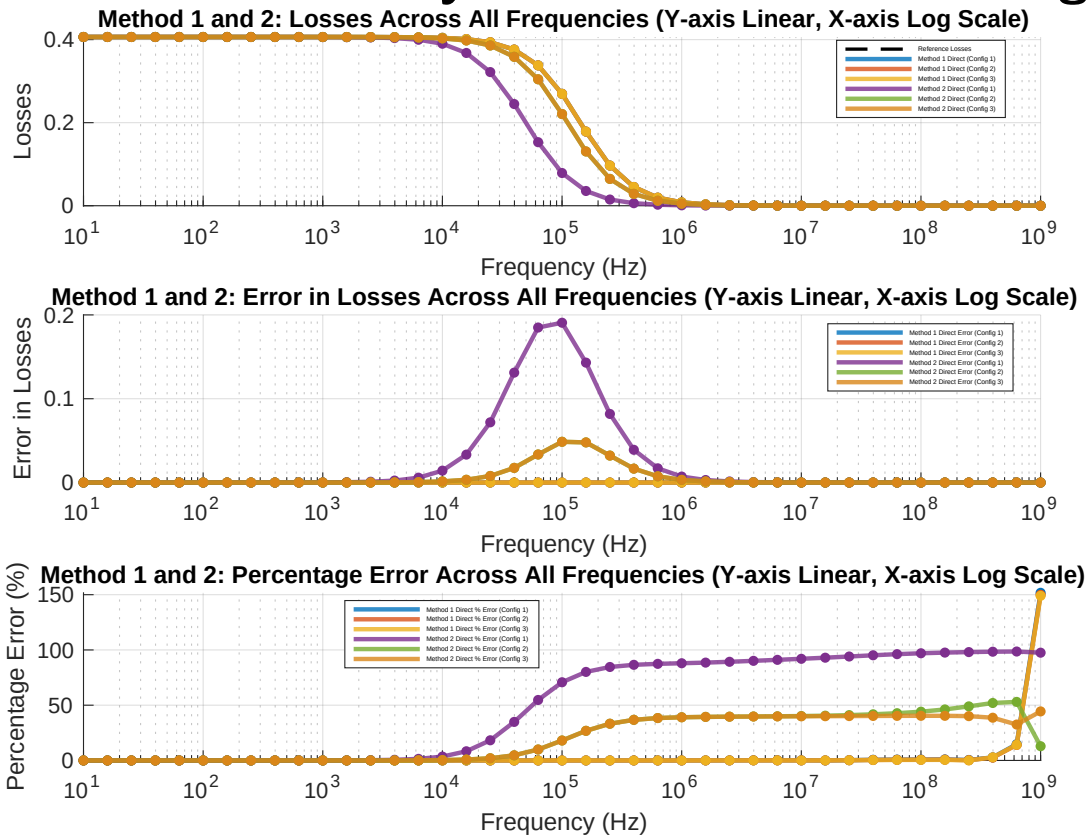

Method 1 and 2 Summary Losses Errors Percentage LogLog

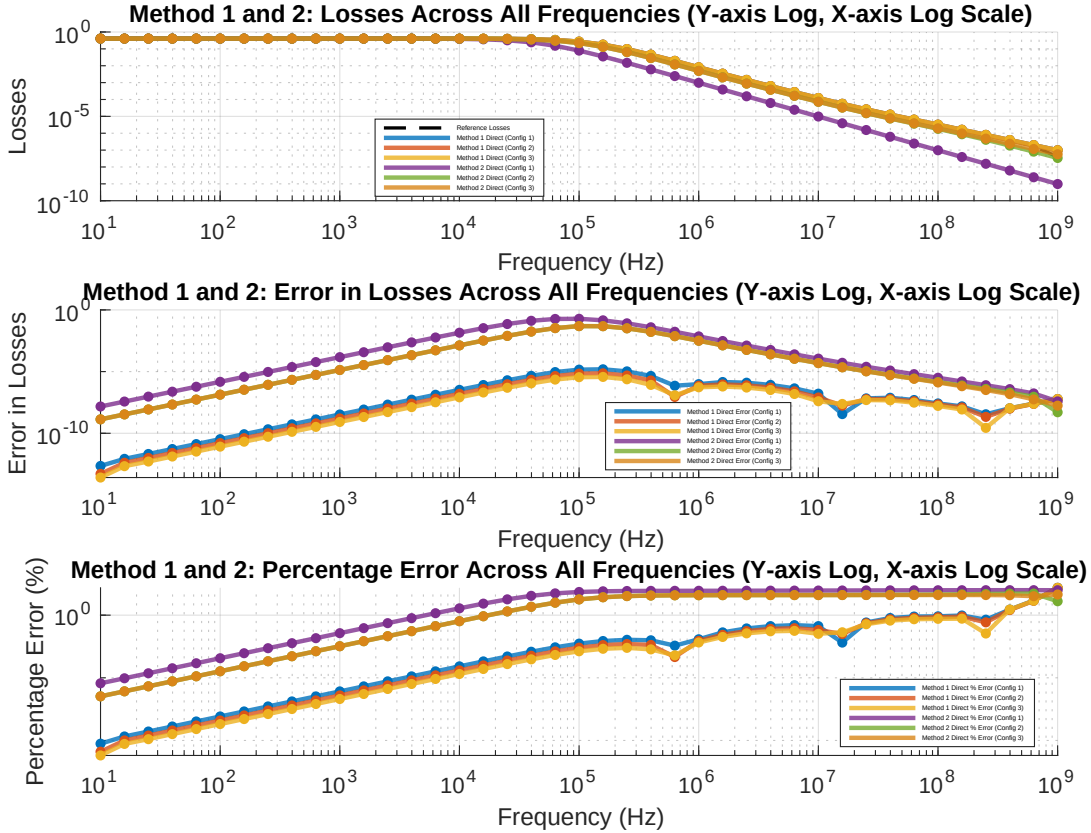

Combined Analysis of Method 1 and Method 2:

- Both methods demonstrate an increase in errors as the frequency rises, with significant discrepancies becoming apparent beyond 10^5 Hz.
- **Mesh Refinement:** Refining the mesh by increasing the number of grid points (nx, ny) consistently reduces errors in both methods, highlighting the importance of mesh resolution.
- **Performance Comparison:**
  - Both methods, when using a finer mesh, yield satisfactory results up to 10^5 Hz. However, at higher frequencies, the errors increase significantly. This is primarily because, as the losses decrease, even minor errors result in high percentage discrepancies.

Application of Non-Uniform Mesh to Method 2:

- While Method 2 currently utilizes a uniform mesh configuration, there is potential to enhance its accuracy and performance by implementing a non-uniform mesh similar to that used in Method 1.
- A non-uniform mesh, with higher grid density in regions of interest where current densities are significant, could result in more precise simulations with lower computational costs compared to uniformly refined meshes.

References I


D. P. Morisco, S. Kurz, H. Rapp, and A. Möckel, "A hybrid modeling approach for current diffusion in rectangular conductors," *IEEE Transactions on Magnetics*, vol. 55, no. 9, pp. 1–9, 2019.


C. R. Paul, *Inductance: Loop and Partial*.
Hoboken, NJ: John Wiley & Sons, 2010.